Excitation-Wavelength-Dependent Photophysics of a Torsionally Disordered Push–Pull Dye

Fureraj, Ina; Wega, Johannes; Balanikas, Vangelis; Pamungkas, Krisna; Sakai, Naomi; Matile, Stefan; Vauthey, Eric

How to cite

FURERAJ, Ina et al. Excitation-Wavelength-Dependent Photophysics of a Torsionally Disordered Push–Pull Dye. In: The journal of physical chemistry letters, 2024, vol. 15, p. 7857–7862. doi: 10.1021/acs.jpclett.4c01840

This publication URL: https://archive-ouverte.unige.ch/unige:179062

Publication DOI: 10.1021/acs.jpclett.4c01840

Excitation-Wavelength Dependent Photophysics of a Torsionally Disordered Push-Pull Dye

Ina Fureraj,[†] Johannes Wega,[†] Evangelos Balanikas,[†] Khurnia Krisna Puji Pamungkas,[‡] Naomi Sakai,[‡] Stefan Matile,[*,‡] and Eric Vauthey[*,†]

[†]*Department of Physical Chemistry, University of Geneva, CH-1211 Geneva, Switzerland.*
[‡]*Department of Organic Chemistry, University of Geneva, CH-1211 Geneva, Switzerland.*

E-mail: stefan.matile@unige.ch; eric.vauthey@unige.ch

Abstract

The torsional disorder of conjugated dyes in the electronic ground state can lead to inhomogeneous broadening of the $S_1 \leftarrow S_0$ absorption band, allowing for selective photoexcitation of molecules with different amounts of distorsion. Here, we investigate how this affects electronic transitions to upper excited states. We show that torsion of a core-alkynylated push-pull dye can have opposite effects on the oscillator strength of its lowest-energy transitions. Consequently, photoselection of planar and twisted molecules can be achieved by exciting in distinct absorption bands. Whereas this has limited effect in liquids due to fast planarisation of the excited molecules, it strongly affects the overall photophysics in a polymeric environment, where torsional motion is hindered, allowing for the photoselection of molecules with different fluorescence quantum yields and intersystem-crossing dynamics.

TOC Graphic

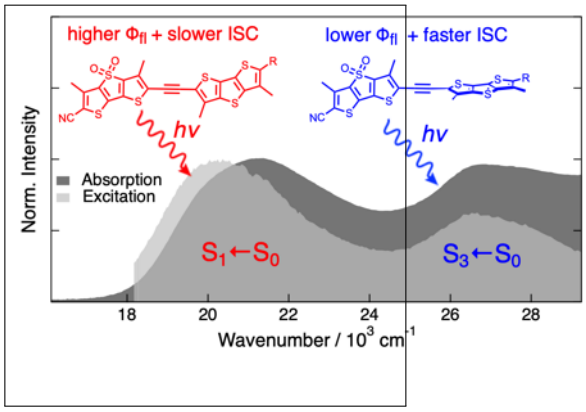

Most conjugated polymers as well as many conjugated dyes are characterised by a significant flexibility for torsion.[1–7] This is particularly true for those containing one or several ethynyl units.[8–20] In the electronic excited state, however, the torsional barrier is usually larger, due to the enhanced conjugation enabled in the planar geometry. The dependence of the S_1-S_0 gap on the twist angle results in an inhomogeneous broadening of the absorption band, i.e, this band is the sum of the slightly different absorption bands associated with each subpopulations.[21] As a consequence, the absorption spectrum of these compounds is usually broad at room temperature, whereas the emission spectrum is narrower and structured as a result of a well-defined excited-state geometry.[9,12,14,18] This allows for the photoselection of molecules with different amount of torsional disorder, planar geometries being selected upon red-edge excitation and disordered structures being preferentially excited at shorter wavelengths. This has been exploited in several studies, which demonstrated the excitation-wavelength dependence of various processes, such as structural relaxation,[15,18] intramolecular energy and charge transfer,[22] as well as singlet fission.[23] In some cases, twisting around the spacer can additionally affect the coupling between two linked chromophoric units. This leads to distinct absorption spectra for the planar and twisted conformations, and enables straightforward photoselection.[24,25]

Here, we investigate how the torsional coordinate affects not only the $S_1 \leftarrow S_0$ transition but also transitions to upper excited states. For this, we use a core-alkynylated push-pull dye (Figure 1A), which was designed to act as mechanophore for sensing lateral compression,[26] as well as rotor for reporting on viscosity. Recent investigation of its excited-state dynamics upon $S_1 \leftarrow S_0$ excitation in solution revealed some photoselectivity, but with minor effect on the overall photophysics.[27] We show here that torsion influences not only the energy but also the oscillator strength of the transitions to the lowest singlet excited states. This allows for efficient photoselection of molecules with different geometries, not by exciting at various

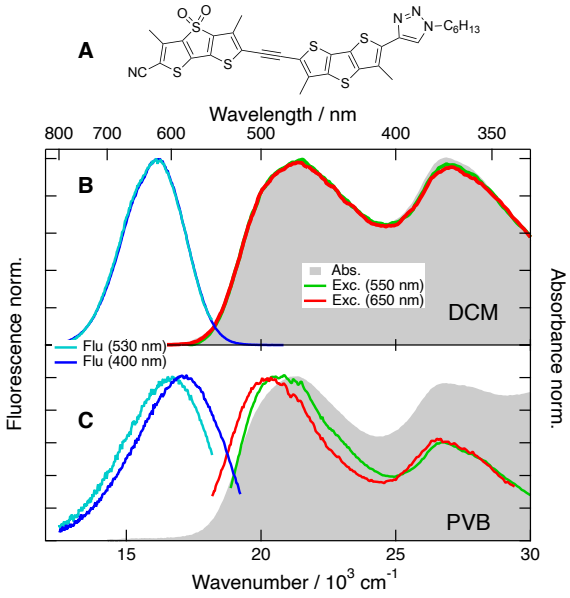

Figure 1: Structure of the core-alkynylated dye (A) and stationary absorption (grey shading), emission (blue lines) and fluorescence excitation spectra (red and green lines) in dichloromethane (DCM, B) and in a polyvinylbutyral (PVB) film (C).

wavelengths throughout the $S_1 \leftarrow S_0$ band, but upon excitation in distinct absorption bands. Whereas such photoselection has limited effect on the photophysics in liquids, it has a major impact in rigid media where relaxation along the torsional coordinate is hindered.

Figure 1 reveals that, contrary to liquid solutions, the fluorescence excitation spectrum of the dye in a polyvinylbutyral (PVB) film departs markedly from the absorption spectrum, and depends on the wavelength at which emission is monitored. The intensity ratio of the low- and high-energy bands, further on called red and blue bands, is significantly larger in the excitation spectra. This points to a fluorescence quantum yield decreasing by a factor of about two upon excitation in the blue band. The red shift of the excitation spectra reveals that the molecules absorbing on the low-energy side of the red band have the highest fluorescence quantum yield. The dependence of the emission spectrum on the excitation wavelength also points to distinct subpopulations. These results can be rationalised with the help of gas-phase

quantum-chemical calculations at the time-dependent density functional theory (TD-DFT, CAM-B3LYP/6-31g(d,p)) level summarised in (Figure 2A, S1 and S2). As discussed previously,[27] full rotation around the ethynyl spacer is possible in the electronic ground state at room temperature, whereas a planar S_1 state is predicted at thermal equilibrium. This difference between the ground and excited state energies leads to a pronounced dependence of the S_1-S_0 gap on the torsion angle and, thus an inhomogeneous broadening of the red band, with its low-energy side due to the absorption of planar molecules.

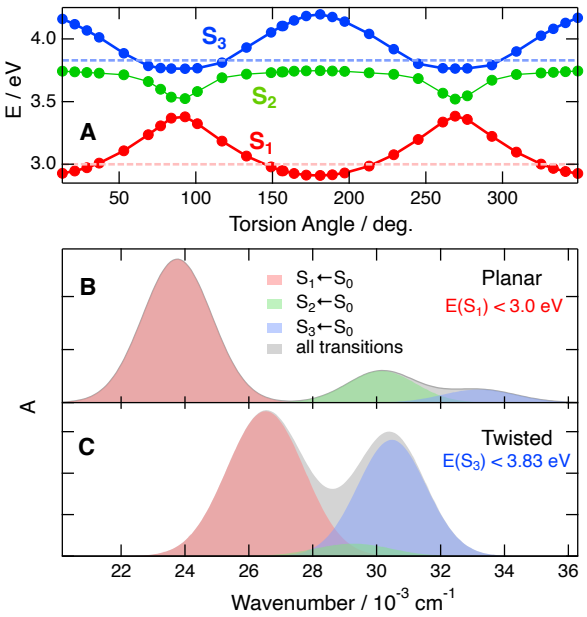

Figure 2: A) Vertical energies of the three lowest singlet excited state determined from TD-DFT calculations (CAM-B3LYP/6-31g(d,p)) in the gas phase; B,C) Simulated absorption spectra of the planar and twisted subpopulations based on the quantum-chemical calculations. For the planar subpopulation, only molecules with an S_1 energy below 3 eV (red dashed line in panel A) were selected. For the twisted subpopulation, only molecules with an S_3 energy below 3.83 eV (blue dashed line in panel A) were considered.

Moreover, the calculations predict the oscillator strength of this transition to also depend on torsion and to be the highest in the planar geometry (Figure S2C). This accounts for the difference between the absorption and fluorescence excitation spectra in the red band in PVB (Figure 1). As the ground-state torsional disorder is mostly frozen in rigid media, red-edge excitation selects the planar and most emissive dyes, whereas disordered molecules are excited at shorter wavelengths.

Interestingly, these calculations suggest different dependences on torsion for the $S_1 \leftarrow S_0$ transition and for those from the ground to the S_2 and S_3 states. The twisted geometry should have the lowest energy for both transitions to the upper states (Figures 2A) and, in the case of the $S_3 \leftarrow S_0$ transition, the highest oscillator strength (Figure S2C).

These results were used to simulate the room-temperature absorption spectrum. Figure 2B,C illustrates the absorption spectra of the populations with close to planar and 90°-twisted geometries (see Section S2 for details). The simulations predict that the low-energy side of the red band is mostly due to the $S_1 \leftarrow S_0$ transition of planar dyes, whereas the blue band is dominated by the $S_3 \leftarrow S_0$ transition of twisted molecules. As the latter have also a smaller $S_1 \leftarrow S_0$ oscillator strength, these simulations explain why the fluorescence quantum yield in PVB is significantly smaller upon blue-band than red-band excitation (Figure 1B). The observed increase of the intensity ratio of the red and blue bands upon lowering temperature (Figure S6) is also reproduced by the simulations (Figure S3).

Transient electronic absorption (TA) spectra recorded in benzonitrile (BCN) and dichloromethane (DCM) upon red- and blue-band excitation are compared in Figure 3A and S7, whereas the results of a global analysis of the TA data assuming a series of successive exponential steps,[28,29] are shown in Figure S8. Independently of the excitation wavelength, the early TA spectra are dominated by a positive excited-state absorption (ESA) band centred above 700 nm and three negative bands: one between 550 and 680 nm, which can be attributed to the $S_1 \rightarrow S_0$ stimulated emission (SE), and two below 500 nm, which can be assigned to the bleach of the red and blue bands. Despite these common spectral features, two

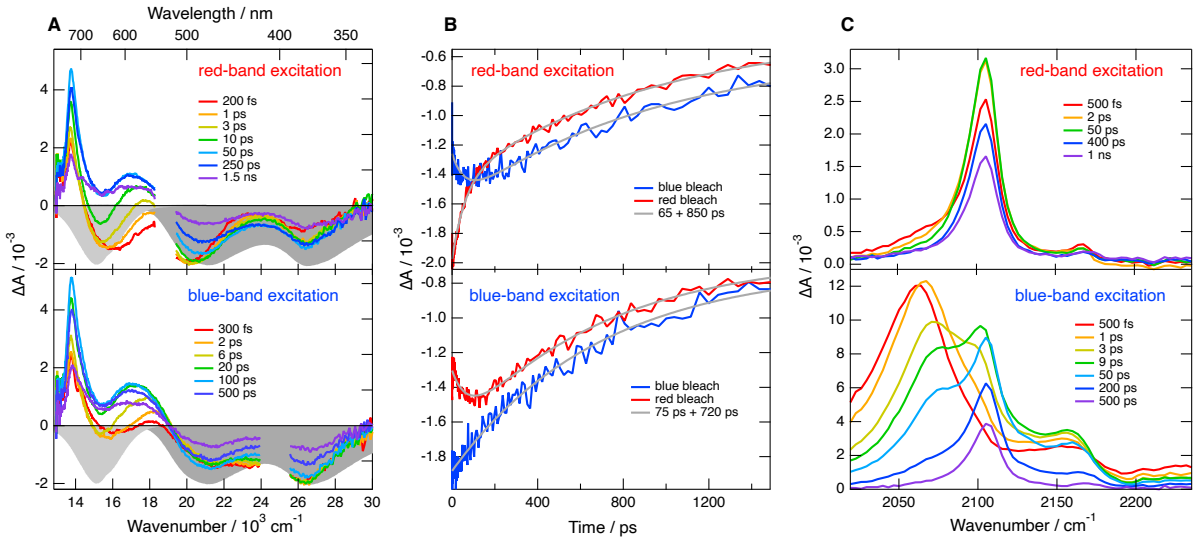

Figure 3: (A) Transient electronic absorption spectra recorded upon red-band (532 nm) and blue-band (400 nm) excitation of the dye in benzonitrile and negative stationary stimulated emission (light grey) and absorption spectra (dark grey). (B) Time profiles at the maximum of the red and blue bleaches taken from the data in the left panels and best bi-exponential fits (grey lines). (C) Transient IR absorption spectra recorded in the −C≡C− and −C≡N stretch region after red- and blue-band excitation in dichloromethane.

main differences, depending on the excitation wavelength, can be observed at early time: 1) the SE band is more pronounced upon red-band excitation, and 2) the red bleach is larger than the blue bleach upon red-band than blue-band excitation and vice-versa. This result is an unambiguous confirmation that photoselection of distinct subpopulations can be achieved upon excitation in the different absorption bands of the dye. The stronger SE and red bleach intensities upon red-band excitation originate from the larger S_1-S_0 oscillator strength of the planar molecules. Similarly, the weaker SE and larger blue bleach upon blue-band excitation confirm that the molecules absorbing the most at these shorter wavelengths have a smaller S_1-S_0 oscillator strength, as expected for twisted geometry.

By contrast, the TA spectra recorded at later times do no longer depend on the excitation wavelength, indicative of a common equilibrium excited state, the planar S_1 state, according to the calculations (Figure 2). The time evolutions of the TA at the red and blue bleach maxima show opposite dependences on the excitation wavelength (Figure 3B and S7). They can be satisfactorily reproduced by the sum of two exponential functions. The fast component can be attributed to reequilibration of the ground-state population along the torsional coordinate after partial depletion of the planar (red-band excitation) or twisted (blue-band excitation) subpopulations.[18,30] Such process can be viewed as the refilling of a spectral hole by spectral diffusion.[31,32] The longer time constant in BCN, ∼70 ps, compared to DCM, 15 ps, can be attributed to higher viscosity of BCN compared to DCM, i.e. 1.25 vs. 0.41 cP at 298 K. This suggests that the motion along the torsional coordinate in the ground state is purely diffusive, as expected for barrier-free large amplitude motion.[33,34] The slower component, which is independent of the excitation wavelength, reflects the partial recovery of the ground-state population upon fluorescence and internal conversion from the S_1 state. As discussed previously,[27] the S_1 state undergoes intersystem-crossing (ISC) on the 1-2 ns timescale with an efficiency of the order of 50%.

Transient IR absorption measurements in the −C≡C− and −C≡N stretch regions reveal a strong dependence of the spectral dynamics on the excitation wavelength (Figure 3C and S12). Upon red-band excitation, the transient spec-

tra consists of an intense band at 2106 cm^{-1} and a weak one at 2167 cm^{-1} associated with the $-C\equiv C-$ and $-C\equiv N$ stretch modes of the dye in the S_1 state, respectively. Apart from a fast decay of the low-frequency shoulder of the $-C\equiv C-$ band, little spectral dynamics is visible. By contrast, the early spectra upon blue-band excitation are dominated by a broad band around 2060 cm^{-1} and transform on multiple timescales to the same spectrum as that measured upon red-band excitation. Much less spectral dynamics can be observed with the $-C\equiv N$ stretching band, apart from an increase of its relative intensity at early time. According to quantum-chemistry calculations, the $-C\equiv C-$ stretching frequency in the S_1 state decreases by about 100 cm^{-1} upon going from the planar to the twisted geometry (Figure S4), whereas it changes by less than 2 cm^{-1} in the ground state. Therefore, the early transient IR band around 2060 cm^{-1} can be attributed to twisted molecules in the excited state and the subsequent spectral dynamics to planarisation and vibrational relaxation.[35] The early increase of the relative intensity of the $-C\equiv N$ band can also be accounted for by planarisation. According to the calculations (Figure S1), electronic excitation in the twisted structure is mostly localised on the electron-donating sub-unit and should thus not significantly affect the cyano group located on the electron-accepting sub-unit, hence the relatively weak transient band.

Transient electronic absorption measurements on the fs-ps and ns-μs timescales were also carried out in PVB (Figures 4 and S9-S11), where torsional motion is expected to be hindered. Contrary to liquids, the effect of excitation wavelength does not vanish after a few tens of ps, but remains visible up to the μs timescale, where only the T_1 state is populated. As illustrated in Figures 4C and S10, the relative magnitude of the red bleach remains larger upon red than blue-band excitation during the entire triplet state lifetime.

The decay of the S_1 state, estimated from the decrease of the SE band, is markedly faster upon blue than red-band excitation. It occurs on multiple timescales with the main component associated with a 250 vs. 640 ps time constant (Figure (S9)). Given the relatively small changes of the bleach intensity, the decay of the S_1 state is predominantly due to ISC to the T_1 state.

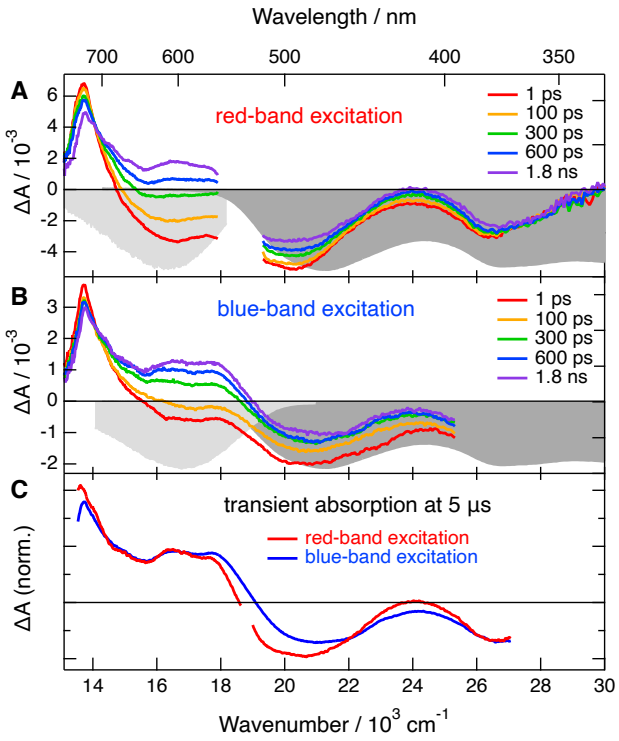

Figure 4: Transient electronic absorption spectra recorded upon (A) red- band (532 nm) and (B) blue-band (370 nm) excitation of the dye in a PVB film and negative stationary stimulated emission (light grey) and absorption spectra (dark grey).(C) Comparison of the transient absorption recorded in PVB 5 μs after 532 and 355 nm excitation.

These results in a rigid environment point to a strong dependence of the ISC dynamics on whether excitation is carried out in the red or the blue band. This suggests that the twisted dyes undergo faster ISC. This is in agreement with previous observations of enhanced ISC upon out-of-plane distortion.[36–41] According to TD-DFT calculations, the three lowest triplet states of the dye are located below the S_1 state, independently of the torsion angle (Figure S5). To estimate how torsion affects ISC, the spin-orbit coupling (SOC) between the S_1 state and the three lowest triplet states was calculated for the planar and the 90° twisted geometries.[42,43] The results, summarised in Table S1, reveal an

increase by a factor 6, i.e. from 1.8 to 10.7 cm^{-1}, of the SOC between the S_1 and the T_3 states. Considering that the ISC rate constant scales with the square of the SOC, these calculations predict a considerable acceleration of the ISC upon distortion. In view of the charge-transfer character of the S_1 state and the tendency of the excitation to localise on either the donor or the acceptor subunit in the 90°-twisted geometry (Figure S1), this enhanced SOC is reminiscent of the so-called spin-orbit charge-transfer (SOCT) ISC mechanism responsible for triplet recombination after photoinduced charge separation in electron donor-acceptor dyads.[44–50]

Until now, photoselection of subpopulations with different amounts of torsional disorder was carried out by tuning the excitation wavelength within the inhomogeneously broadened $S_1 \leftarrow S_0$ transition. Here, we show that torsion not only affects the energy of this transition but also influences its oscillator strength as well as those of transitions to upper states. This allows for the photoselection of subpopulations with a given geometry upon exciting distinct absorption bands. Whereas such photoselection only affects the early excited-state dynamics in liquid environments, it strongly impacts the overall photophysics in rigid media, allowing for the selective excitation of molecules with a fluorescence quantum yield varying by a factor of more than two and with significantly different ISC dynamics. Such behaviour might be rather common with core-alkynylated electron donor-acceptor dyads and deserves further attention as it could be advantageously exploited for sensing and/or theranostic applications.

Acknowledgement Financial support from the Swiss National Science Foundation (grants 200020-204175 and 200020-184607) and the University of Geneva is acknowledged. The computations were performed at University of Geneva using Baobab HPC service.

Supporting Information Available

Experimental details, additional results: quantum chemical calculations, stationary spectra, transient electronic and vibrational absorption spectra, results from global analysis.

Additional note

All data can be downloaded from https://doi.org/10.26037/yareta:vzkfwgcqkfdanpv47mopub3nte

References

(1) Grozema, F. C.; van Duijnen, P. T.; Berlin, Y. A.; Ratner, M. A.; Siebbeles, L. D. A. Intramolecular Charge Transport along Isolated Chaing of Conjugated Polymers. Effect of Torsional Disorder and Polymerization Defects. *J. Phys. Chem. B* **2002**, *106*, 7791–7795.

(2) Bjorgaard, J. A.; Köse, M. E. Theoretical Study of Torsional Disorder in Poly(3-alkylthiophene) Single Chains: Intramolecular Charge-Transfer Character and Implications for Photovoltaic Properties. *J. Phys. Chem. A* **2013**, *117*, 3869–3876.

(3) McLeod, J. A.; Pitman, A. L.; Kurmaev, E. Z.; Finkelstein, L. D.; Zhidkov, I. S.; Savva, A.; Moewes, A. Linking the HOMO-LUMO Gap to Torsional Disorder in P3HT/PCBM Blends. *J. Chem. Phys.* **2015**, *143*, 224704.

(4) Simine, L.; Rossky, P. J. Relating Chromophoric and Structural Disorder in Conjugated Polymers. *J. Phys. Chem. Lett.* **2017**, *8*, 1752–1756.

(5) Park, K. H.; Son, S. Y.; Kim, J. O.; Kang, G.; Park, T.; Kim, D. Role of Disorder in the Extent of Interchain Delocalization and Polaron Generation in Polythiophene Crystalline Domains. *J. Phys. Chem. Lett.* **2018**, *9*, 3173–3180.

(6) Beer, P.; Reichstein, P. M.; Schötz, K.; Raithel, D.; Thelakkat, M.; Köhler, J.; Panzer, F.; Hildner, R. Disorder in P3HT Nanoparticles Probed by Optical Spectroscopy on P3HT-b-PEG Micelles. *J. Phys. Chem. A* **2021**, *125*, 10165–10173.

(7) Dimitriev, O. P. Dynamics of Excitons in Conjugated Molecules and Organic Semiconductor Systems. *Chem. Rev.* **2022**, *122*, 8487–8593.

(8) Bunz, U. H. F. Poly(aryleneethynylene)s: Syntheses, Properties, Structures, and Applications. *Chem. Rev.* **2000**, *100*, 1605–1644.

(9) Sluch, M. I.; Godt, A.; Bunz, U. H. F.; Berg, M. A. Excited-State Dynamics of Oligo(p-phenyleneethynylene): Quadratic Coupling and Torsional Motions. *J. Am. Chem. Soc.* **2001**, *123*, 6447–6448.

(10) Beeby, A.; Findlay, K.; Low, P. J.; Marder, T. B. A Re-evaluation of the Photophysical Properties of 1,4-Bis(phenylethynyl)benzene: A Model for Poly(phenyleneethynylene). *J. Am. Chem. Soc.* **2002**, *124*, 8280–8284.

(11) Beeby, A.; Findlay, K. S.; Low, P. J.; Marder, T. B.; Matousek, P.; Parker, A. W.; Rutter, S. R.; Towrie, M. Studies of the S1 State in a Prototypical Molecular Wire using Picosecond Time-Resolved Spectroscopies. *Chem. Commun.* **2003**, 2406–7.

(12) Magyar, R. J.; Tretiak, S.; Gao, Y.; Wang, H.-L.; Shreve, A. P. A Joint Theoretical and Experimental Study of Phenylene–Acetylene Molecular Wires. *Chem. Phys. Lett.* **2005**, *401*, 149–156.

(13) Liu, L. T.; Yaron, D.; Sluch, M. I.; Berg, M. A. Modeling the Effects of Torsional Disorder on the Spectra of Poly- and Oligo-(p-phenyleneethynylenes). *J. Phys. Chem. B* **2006**, *110*, 18844–18852.

(14) Duvanel, G.; Grilj, J.; Schuwey, A.; Gossauer, A.; Vauthey, E. Ultrafast Excited-State Dynamics of Phenyleneethynylene Oligomers in Solution. *Photochem. Photobiol. Sci.* **2007**, *6*, 956–963.

(15) Roy, K.; Kayal, S.; Ravi Kumar, V.; Beeby, A.; Ariese, F.; Umapathy, S. Understanding Ultrafast Dynamics of Conformation Specific Photo-Excitation: A Femtosecond Transient Absorption and Ultrafast Raman Loss Study. *J. Phys. Chem. A* **2017**, *121*, 6538–6546.

(16) Peeks, M. D.; Tait, C. E.; Neuhaus, P.; Fischer, G. M.; Hoffmann, M.; Haver, R.; Cnossen, A.; Harmer, J. R.; Timmel, C. R.; Anderson, H. L. Electronic Delocalization in the Radical Cations of Porphyrin Oligomer Molecular Wires. *J. Am. Chem. Soc.* **2017**, *139*, 10461–10471.

(17) Paéz-Pérez, M.; López-Duarte, I.; Vyšniauskas, A.; Brooks, N. J.; Kuimova, M. K. Imaging Non-Classical Mechanical Responses of Lipid Membranes using Molecular Rotors. *Chem. Sci.* **2021**, *12*, 2604–2613.

(18) Fureraj, I.; Budkina, D. S.; Vauthey, E. Torsional Disorder and Planarization Dynamics: 9,10-Bis(phenylethynyl)anthracene as a Case Study. *Phys. Chem. Chem. Phys.* **2022**, *24*, 25979–25989.

(19) Ringström, R.; Schroeder, Z. W.; Mencaroni, L.; Chabera, P.; Tykwinski, R. R.; Albinsson, B. Triplet Formation in a 9,10-Bis(phenylethynyl)anthracene Dimer and Trimer Occurs by Charge Recombination Rather than Singlet Fission. *J. Phys. Chem. Lett.* **2023**, *14*, 7897–7902.

(20) Alomar, S. A.; Gutiérrez-Arzaluz, L.; Nadinov, I.; He, R.; Wang, X.; Wang, J.-X.; Jia, J.; Shekhah, O.; Eddaoudi, M.; Alshareef, H. N. et al. Tunable Photoinduced Charge Transfer at the Interface between Benzoselenadiazole-Based MOF

Linkers and Thermally Activated Delayed Fluorescence Chromophore. *J. Phys. Chem. B* **2023**, *127*, 1819–1827.

(21) Nitzan, A. *Chemical Dynamics in Condensed Phases*; Oxford University Press: Oxford, 2006.

(22) Albinsson, B.; Mårtensson, J. Long-Range Electron and Excitation Energy Transfer in Donor-Bridge-Acceptor Systems. *J. Photochem. Photobiol. C* **2008**, *9*, 138–155.

(23) Ringström, R.; Edhborg, F.; Schroeder, Z. W.; Chen, L.; Ferguson, M. J.; Tykwinski, R. R.; Albinsson, B. Molecular Rotational Conformation Controls the Rate of Singlet Fission and Triplet Decay in Pentacene Dimers. *Chem. Sci.* **2022**, *13*, 4944–4954.

(24) Winters, M.; Kärnbratt, J.; Blades, H.; Wilson, C.; Frampton, M.; Anderson, H.; Albinsson, B. Control of Electron Transfer in a Conjugated Porphyrin Dimer by Selective Excitation of Planar and Perpendicular Conformers. *Chem. Eur. J.* **2007**, *13*, 7385–7394.

(25) Kuimova, M. K.; Balaz, M.; Anderson, H. L.; Ogilby, P. R. Intramolecular Rotation in a Porphyrin Dimer Controls Singlet Oxygen Production. *J. Am. Chem. Soc.* **2009**, *131*, 7948–7949.

(26) Chen, X.-X.; Bayard, F.; Gonzalez-Sanchis, N.; Pamungkas, K. K. P.; Sakai, N.; Matile, S. Fluorescent Flippers: Small-Molecule Probes to Image Membrane Tension in Living Systems. *Angew. Chem. Int. Ed.* **2023**, *62*, e202217868.

(27) Pamungkas, K. K. P.; Fureraj, I.; Assies, L.; Sakai, N.; Mercier, V.; Chen, X.-X.; Vauthey, E.; Matile, S. Core-Alkynylated Fluorescent Flippers: Altered Ultrafast Photophysics to Track Thick Membranes. *Angew. Chem. Int. Ed.* **2024**, *23*, e202406204.

(28) van Stokkum, I. H. M.; Larsen, D. S.; van Grondelle, R. Global and Target Analysis of Time-Resolved Spectra. *Biochim. Biophys. Acta, Bioenerg.* **2004**, *1657*, 82–104.

(29) Beckwith, J. S.; Rumble, C. A.; Vauthey, E. Data Analysis in Transient Electronic Spectroscopy – an Experimentalist's View. *Int. Rev. Phys. Chem.* **2020**, *39*, 135–216.

(30) Sissaoui, J.; Budkina, D. S.; Vauthey, E. Torsional Disorder, Symmetry Breaking, and the Crystal Violet Shoulder Controversy. *J. Phys. Chem. Lett.* **2023**, *14*, 5602–5606.

(31) Friedrich, J.; Haarer, D. Photochemical Hole Burning: A Spectroscopic Study of Relaxation Processes in Polymers and Glasses. *Angew. Chem. Int. Ed.* **1984**, *23*, 113–140.

(32) Basché, T.; Ambrose, W. P.; Moerner, W. E. Optical Spectra and Kinetics of Single Impurity Molecules in a Polymer: Spectral Diffusion and Persistent Spectral Hole Burning. *J. Opt. Soc. Am. B* **1992**, *9*, 829–836.

(33) Kramers, H. A. Brownian Motion in a Field of Force and the Diffusion Model of Chemical Reactions. *Physica* **1940**, *7*, 284–304.

(34) Bagchi, B.; Fleming, G. R.; Oxtoby, D. W. Theory of Electronic Relaxation in Solution in the Absence of an Activation Barrier. *J. Chem. Phys.* **1983**, *78*, 7375–7385.

(35) Soederberg, M.; Dereka, B.; Marrocchi, A.; Carlotti, B.; Vauthey, E. Ground-state Structural Disorder and Excited-state Symmetry Breaking in a Quadrupolar Molecule. *J. Phys. Chem. Lett.* **2019**, *10*, 2944–2948.

(36) Arbogast, J. W.; Foote, C. S. Photophysical properties of C70. *J. Am. Chem. Soc.* **1991**, *113*, 8886–8889, doi: 10.1021/ja00023a041.

(37) Lewis, F. D.; Zuo, X. Activated Decay Pathways for Planar vs Twisted Singlet Phenylalkenes. *J. Am. Chem. Soc.* **2003**, *125*, 8806–8813.

(38) Menning, S.; Krämer, M.; Duckworth, A.; Rominger, F.; Beeby, A.; Dreuw, A.; Bunz, U. H. F. Bridged Tolanes: A Twisted Tale. *J. Org. Chem.* **2014**, *79*, 6571–6578.

(39) Nagarajan, K.; Mallia, A. R.; Muraleedharan, K.; Hariharan, M. Enhanced Intersystem Crossing in Core-Twisted Aromatics. *Chem. Sci.* **2017**, *8*, 1776–1782.

(40) Mahmood, Z.; Sukhanov, A. A.; Rehmat, N.; Hu, M.; Elmali, A.; Xiao, Y.; Zhao, J.; Karatay, A.; Dick, B.; Voronkova, V. K. Intersystem Crossing and Triplet-State Property of Anthryl- and Carbazole-[1,12]fused Perylenebisimide Derivatives with a Twisted π-Conjugation Framework. *J. Phys. Chem. B* **2021**, *125*, 9317–9332.

(41) Saleh, N.; Sucre-Rosales, E.; Zinna, F.; Besnard, C.; Vauthey, E.; Lacour, J. Axially-Chiral Boramidine for Detailed (Chir)optical Studies. *Chem. Sci.* **2024**, *15*, 6530–6535.

(42) de Souza, B.; Farias, G.; Neese, F.; Izsák, R. Predicting Phosphorescence Rates of Light Organic Molecules Using Time-Dependent Density Functional Theory and the Path Integral Approach to Dynamics. *J. Chem. Theory Comput.* **2019**, *15*, 1896–1904.

(43) Neese, F. Software Update: The ORCA Program System—Version 5.0. *WIREs Comput. Mol. Sci.* **2022**, *12*, e1606.

(44) Okada, T.; Karaki, I.; Matsuzawa, E.; Mataga, N.; Sakata, Y.; Misumi, S. Ultrafast Intersystem Crossing in some Intramolecular Heteroexcimers. *J. Phys. Chem.* **1981**, *85*, 3957–3960.

(45) Wasielewski, M. R.; Johnson, D. G.; Svec, W. A.; Kersey, K. M.; Minsek, D. W. Achieving High Quantum Yield Charge Separation in Porphyrin-Containing Donor-Acceptor Molecules at 10 K. *J. Am. Chem. Soc.* **1988**, *110*, 7219–7221.

(46) Ziessel, R.; Allen, B.; Rewinska, D.; Harriman, A. Selective Triplet-State Formation during Charge Recombination in a Fullerene/Bodipy Molecular Dyad (Bodipy=Borondipyrromethene). *Chem. Eur. J.* **2009**, *15*, 7382–7393.

(47) Letrun, R.; Lang, B.; Yushchenko, O.; Wilcken, R.; Svechkarev, D.; Kolodieznyi, D.; Riedle, E.; Vauthey, E. Excited-State Dynamics of a Molecular Dyad with Two Orthogonally-Oriented Fluorophores. *Phys. Chem. Chem. Phys.* **2018**, *20*, 30219–20230.

(48) Das, S.; Thornbury, W. G.; Bartynski, A. N.; Thompson, M. E.; Bradforth, S. E. Manipulating Triplet Yield through Control of Symmetry-Breaking Charge Transfer. *J. Phys. Chem. Lett.* **2018**, *9*, 3264–3270.

(49) Dong, Y.; Sukhanov, A. A.; Zhao, J.; Elmali, A.; Li, X.; Dick, B.; Karatay, A.; Voronkova, V. K. Spin–Orbit Charge-Transfer Intersystem Crossing (SOCT-ISC) in Bodipy-Phenoxazine Dyads: Effect of Chromophore Orientation and Conformation Restriction on the Photophysical Properties. *J. Phys. Chem. C* **2019**, *123*, 22793–22811.

(50) Liu, D.; El-Zohry, A. M.; Taddei, M.; Matt, C.; Bussotti, L.; Wang, Z.; Zhao, J.; Mohammed, O. F.; Di Donato, M.; Weber, S. Long-Lived Charge-Transfer State Induced by Spin-Orbit Charge Transfer Intersystem Crossing (SOCT-ISC) in a Compact Spiro Electron Donor/Acceptor Dyad. *Ang. Chem. Int. Ed.* **2020**, *59*, 11591–11599.